Wuhan University Journal of Natural Sciences

XXXX, Vol.XX No.XX

Article ID 1007-1202(XXXX)XX-0001-08 DOI https://doi.org/10.1051/wujns/XXXXXXXX001

Cite this article: LIU Changfu.New Coherent Structures and Chaotic Patterns for the (2+1)-Dimensional Boiti-Leon-Pempinelli Equation[J]. Wuhan University Journal of Natural Sciences, DOI: https://doi.org/10.1051/wujns/XXXXXXXX001.

New Coherent Structures and Chaotic Patterns for the (2+1)-Dimensional Boiti-Leon-Pempinelli Equation

LIU Changfu

School of Artificial Intelligence, Wenshan University, Wenshan 663099, Yunnan, China

Abstract: The (2+1)-dimensional Boiti-Leon-Pempinelli (BLP) equation is integrable and admits a wide class of coherent structures beyond classical solitons, but such structures are difficult to derive systematically. Combining the auxiliary equation mapping method with the homogeneous balance method, we obtain variable separation solutions that contain two arbitrary functions. These functions allow breather double solitons, symmetric breather solitons and double-period waves to be constructed within one scheme. Analysis of the associated potential field $w(x,y,t)$ further gives fractal rogue waves, fractal dromions and chaotic patterns generated by singular manifolds. The results relate the choice of arbitrary functions directly to the resulting dynamics and clarify the coherence mechanisms of the BLP system.

Key words: (2+1)-dimensional Boiti-Leon-Pempinelli equation; auxiliary equation mapping method; variable separation solutions; coherent structures; chaotic patterns

CLC number: O175.29

0 Introduction

Nonlinear partial differential equations (PDEs) remain central to the description of complex physical systems in fluid dynamics, plasma physics and nonlinear optics. Among these models, the (2+1) -dimensional Boiti-Leon-Pempinelli (BLP) equation is a prototypical integrable system, since it admits a wide range of coherent structures. These localized and stable structures, which often behave like solitons, are central to the description of nonlinear wave dynamics.

Originally formulated by Boiti *et al*[1] to characterize long-wave propagation in (2+1)-dimensional space, the BLP system is given by

$$\begin{cases} u_{yt}-(u^2-u_x)_{xy}-2v_{xxx}=0, \\ v_t-v_{xx}-2uv_x=0. \end{cases} \tag{1}$$

which describes the evolution of the horizontal velocity component of water waves propagating in the $x-y$ plane in a narrow channel of constant depth. It is also regarded as a (2+1)-dimensional generalization of the sinh-Gordon equa-

Received date: 2025-11-01 © Wuhan University 2026

Foundation item: Supported by the National Natural Science Foundation of China (12261053) and the Scientific Research Foundation of Department of Education of Yunnan Province (2022J0946)

Biography: LIU Changfu, male, Professor, research direction: nonlinear partial differential equations. Email: chfuliu@163.com

tion, and is widely used to model weakly nonlinear waves in fluid mechanics. In particular, it describes nonlinear wave-wave interactions[2]. Its integrability and rich mathematical structure have attracted considerable attention. Singh *et al*[3] classified its symmetries and identified the associated invariants; Ghazanfar *et al*[4] derived multi-wave solutions by Hirota bilinearization; Sil and Raja Sekhar[5] analyzed soliton dynamics and nonlocal conservation laws. Methodologically, Radha *et al*[6] used Bäcklund transformations to construct exotic solitonic interactions, Seadawy *et al*[7] developed generalized algebraic methods for analytical wave solutions, and Yang *et al*[8] identified parameter-dependent transitions between soliton excitations and chaotic regimes.

Although much progress has been made[9-32], a complete classification of coherent structures and of their interactions is still lacking. This paper addresses the gap in three ways. First, we derive new exact solutions with the auxiliary equation mapping method. Second, we construct breather-like excitations and doubly periodic waves in a controlled way. Third, we characterize fractal rogue waves and chaotic patterns through a decomposition of the localization functions.

The paper is organized as follows. Section 1 applies the auxiliary equation mapping method to obtain variable separation solutions, which form the basis of the later analysis. Section 2 uses these solutions to construct coherent structures such as breather double solitons and double-period waves. Section 3 examines the local structure of $w(x,y,t)$ for Eqs. (1); with suitable choices of the arbitrary functions we obtain fractal rogue waves, fractal dromions and chaotic patterns. Section 4 concludes the paper.

1 Variable Separation Solutions for Eqs. (1)

In this section, we employ the auxiliary equation mapping method to construct solutions for Eqs. (1). We assume that the solutions take the form given in Ref. [33],

$$\begin{cases} u(x,y,t)=a_0(x,y,t)+\sum\limits_{i=1}^{m}a_i(x,y,t)F^i(\varphi(x,y,t)), \\ v(x,y,t)=b_0(x,y,t)+\sum\limits_{j=1}^{n}b_j(x,y,t)F^j(\varphi(x,y,t)), \end{cases} \tag{2}$$

where $a_0(x,y,t)$, $a_i(x,y,t)$, $b_j(x,y,t)(i=1,\ 2,\ \cdots,\ m;j=1,2,\ \cdots,\ n)$ and $\varphi(x,y,t)$ are to be determined. Here, $F(\varphi(x,y,t))$ satisfies the Riccati equation:

$$F'(\varphi)=F^2(\varphi), \tag{3}$$

with the general solution:

$$F(\varphi(x,y,t))=-\frac{1}{C+\varphi(x,y,t)}, \tag{4}$$

where C is an arbitrary constant. Substituting Eqs. (2) into Eqs. (1) and applying the homogeneous balance method, we determine $m=n=1$. After substituting Eqs. (2) and Eq. (3) into Eqs. (1), we equate the coefficients of $F^i(\varphi(x,y,t))(i=1,\ 2,\ 3,\ 4)$ to zero, leading to the following system of equations:

$$\begin{cases} 6a_1^2\varphi_x\varphi_y-6a_1\varphi_x^2\varphi_y+12b_1\varphi_x^3=0, \\ 4a_0a_1\varphi_x\varphi_y+2a_1(a_{1x}\varphi_y+a_{1y}\varphi_x+a_1\varphi_{xy})-2a_1\varphi_y\varphi_t-2a_{1y}\varphi_x^2+12b_{1x}\varphi_x^2-2a_1\varphi_{xx}\varphi_y-4a_1\varphi_x\varphi_{xy} \\ \quad -4a_{1x}\varphi_x\varphi_y+2a_1a_{1y}\varphi_x+2a_1a_{1x}\varphi_y+12b_1\varphi_x\varphi_{xx}=0, \\ 2a_0(a_{1x}\varphi_y+a_{1y}\varphi_x+a_1\varphi_{xy})+2a_1a_{1\,xy}-a_{1t}\varphi_y+2a_{0y}a_1\varphi_x+2a_{1x}a_{1\,y}+2a_1a_{0x}\varphi_y-2a_{1x}\varphi_{xy}+6b_{1xx}\varphi_x \\ \quad +6b_{1x}\varphi_{xx}-a_{1y}\varphi_{xx}+2b_1\varphi_{xxx}-2a_{1xy}\varphi_x-a_{1xx}\varphi_y-a_1\varphi_{yt}-a_1\varphi_{xxy}-a_{1y}\varphi_t=0, \\ 2a_0a_{1xy}+2b_{1xxx}+2a_1a_{0xy}-2a_{1xxy}-a_{1yt}+2a_{0y}a_{1x}+2a_{0x}a_{1y}=0, \\ 2a_0a_{0xy}-a_{0xxy}-a_{0yt}+2b_{0xxx}+2a_{0y}a_{0x}=0,\ 2a_1b_1\varphi_x+2b_1\varphi_x^2=0, \\ 2a_0b_1\varphi_x-b_1\varphi_t+2a_1b_{1x}+b_1\varphi_{xx}+2b_{1x}\varphi_x=0,\ 2a_0b_{1x}+2a_1b_{0x}+b_{1xx}-b_{1t}=0,\ 2a_0b_{0x}-b_{0t}+b_{0xx}=0. \end{cases} \tag{5}$$

In general, Eqs. (5) cannot be solved analytically. Special solutions can, however, be obtained under particular assumptions.

Case 1 Let $\varphi(x,y,t)=P(x,t)+Q(y)+MP(x,t)Q(y)$. Eqs. (5) yield the following solutions:

$$\begin{cases} a_0(x,y,t)=\dfrac{1}{2}\dfrac{P_t(x,t)-P_{xx}(x,t)}{P_x(x,t)},\ a_1(x,y,t)=-P_x(x,t)(1+MQ(y)), \\ b_0(x,y,t)=H(y),\ b_1(x,y,t)=-Q_y(y)(1+MP(x,t)). \end{cases} \tag{6}$$

where $P(x,t)$, $Q(y)$ and $H(y)$ are arbitrary functions, and M is a constant. Substituting Eqs. (6) and Eq. (4) into Eqs. (2) gives the solutions of Eqs. (1):

$$\begin{cases} u(x,y,t)=\dfrac{1}{2}\dfrac{P_t(x,t)-P_{xx}(x,t)}{P_x(x,t)}+\dfrac{P_x(x,t)(1+MQ(y))}{C+P(x,t)+Q(y)+MP(x,t)Q(y)}, \\ v(x,y,t)=H(y)+\dfrac{Q_y(y)(1+MP(x,t))}{C+P(x,t)+Q(y)+MP(x,t)Q(y)}. \end{cases} \tag{7}$$

The corresponding potential field is written as

$$w(x,y,t)=u_y=v_x=\frac{P_x(x,t)Q_y(y)(MC-1)}{(C+P(x,t)+Q(y)+MP(x,t)Q(y))^2}, \tag{8}$$

where $w(x,y,t)$ is an important physical quantity that provides insight into the dynamics of the fluid and into energy conversion and transmission in electromagnetic systems.

Case 2 Likewise, for $\varphi(x,y,t)=P(x,t)+Q(y,t)+MP(x,t)Q(y,t)$, Eqs. (5) yield:

$$\begin{cases} a_0(x,y,t)=\dfrac{F_t(t)[1+MP(x,t)]-MF(t)[P_{xx}(x,t)-P_t(x,t)]}{2MP_x(x,t)F(t)}, \\ a_1(x,y,t)=-MG(y)F(t)P_x(x,t),\ b_0(x,y,t)=H(y),\ b_1(x,y,t)=-F(t)G_y(y)(1+MP(x,t)),\ Q(y,t)=F(t)G(y)-\dfrac{1}{M}. \end{cases} \tag{9}$$

where $P(x,t)$, $F(t)$, $G(y)$ and $H(y)$ are arbitrary functions, and $M\neq 0$ is a constant.

Substituting Eq. (9) and Eq. (4) into Eqs. (2) gives the solutions of Eqs. (1):

$$\begin{cases} u(x,y,t)=\dfrac{F_t(t)[1+MP(x,t)]-MF(t)[P_{xx}(x,t)-P_t(x,t)]}{2MP_x(x,t)F(t)}+\dfrac{MF(t)G(y)P_x(x,t)}{K+F(t)G(y)+MF(t)G(y)P(x,t)}, \\ v(x,y,t)=H(y)+\dfrac{F(t)G_y(y)(1+MP(x,t))}{K+F(t)G(y)+MF(t)G(y)P(x,t)}. \end{cases} \tag{10}$$

where K is an arbitrary constant.

The corresponding potential field is written as

$$w(x,y,t)=u_y=v_x=\frac{MKP_x(x,t)G_y(y)F(t)}{(K+F(t)G(y)+MF(t)G(y)P(x,t))^2}. \tag{11}$$

To the best of our knowledge, these solutions have not been reported previously.

2 New Coherent Structures for Eqs. (1)

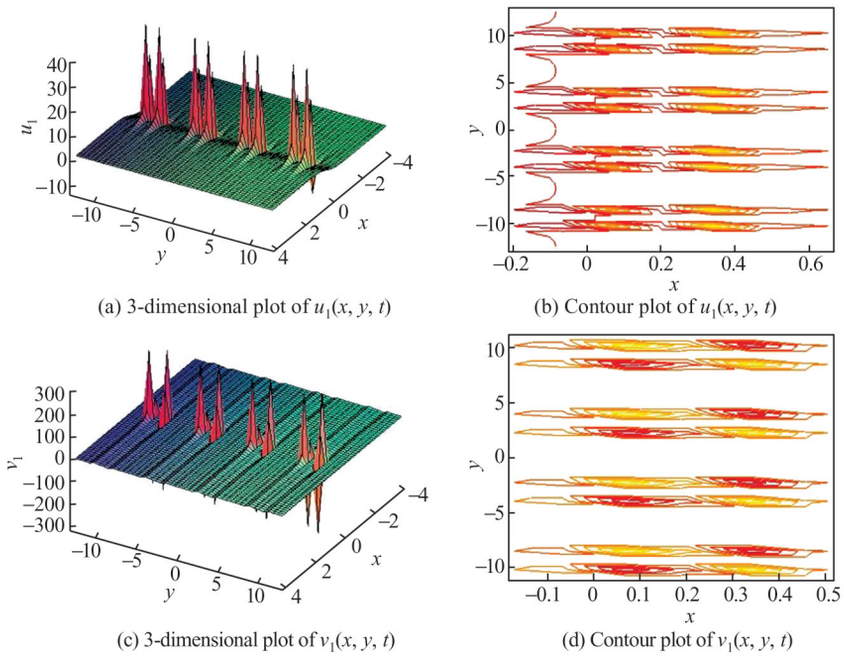
Localized coherent structures of the BLP equation, such as rogue waves, dromions and lump solutions, have been widely reported[5,21]. The solutions in Eqs. (7) and (10), however, contain arbitrary functions, which allow a much wider class of localized structures to be generated. We select three sets of arbitrary functions $P(x,t)$, $F(t)$ and $G(y)$ (or $P(x,t)$ and $Q(y)$) and use them to construct three new types of localized coherent structures, whose interaction behavior is then examined. The results show the extent to which the arbitrary functions can be exploited to generate localized structures and to relate their behavior to specific applications.

2.1 Breather Double Solitons

In Eqs. (7), setting $H(y)=0$, $P(x,t)=C_1\mathrm{e}^{(C_0t+\sqrt{C_0}x)}+C_2\mathrm{e}^{(C_0t-\sqrt{C_0}x)}$ and $Q(y)=\cos(ky+y_0)$ yields the breather double soliton solutions:

$$\begin{cases} u_1(x,y,t)=\sqrt{C_0}\,[C_1\mathrm{e}^{(C_0t+\sqrt{C_0}x)}-C_2\mathrm{e}^{(C_0t-\sqrt{C_0}x)}][1+M\cos(ky+y_0)]/[C+C_1\mathrm{e}^{(C_0t+\sqrt{C_0}x)}+C_2\mathrm{e}^{(C_0t-\sqrt{C_0}x)}+\cos(ky+y_0) \\ \quad +M(C_1\mathrm{e}^{(C_0t+\sqrt{C_0}x)}+C_2\mathrm{e}^{(C_0t-\sqrt{C_0}x)})\cos(ky+y_0)], \\ v_1(x,y,t)=k\sin(ky+y_0)[1+M(C_1\mathrm{e}^{(C_0t+\sqrt{C_0}x)}+C_2\mathrm{e}^{(C_0t-\sqrt{C_0}x)})]/[C+C_1\mathrm{e}^{(C_0t+\sqrt{C_0}x)}+C_2\mathrm{e}^{(C_0t-\sqrt{C_0}x)}+\cos(ky+y_0) \\ \quad +M(C_1\mathrm{e}^{(C_0t+\sqrt{C_0}x)}+C_2\mathrm{e}^{(C_0t-\sqrt{C_0}x)})\cos(ky+y_0)]. \end{cases} \tag{12}$$

Figure 1 shows a breather double soliton formed by the interaction of the double soliton $P(x,t)=2\mathrm{e}^{(4t+2x)}+4\mathrm{e}^{(4t-2x)}$ with the periodic wave $Q(y)=\cos(y)$. The solution is localized and keeps its pulse-like profile as it propagates.



(a) 3-dimensional plot of $u_1(x, y, t)$ (b) Contour plot of $u_1(x, y, t)$

(c) 3-dimensional plot of $v_1(x, y, t)$ (d) Contour plot of $v_1(x, y, t)$

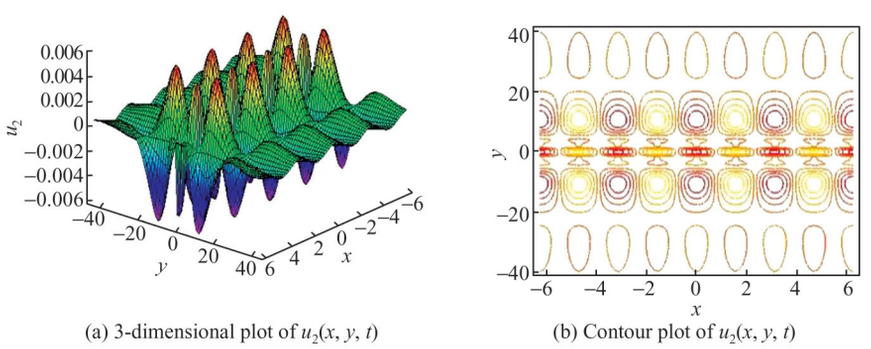
Fig. 1 Plots of $u_1(x,y,t)$ and $v_1(x,y,t)$ when $C_0=4$, $C_1=2$, $C_2=4$, $C=100$, $M=2$, $k=1$, $y_0=0$ and $t=1$ in Eqs. (12)

2.2 Symmetric Breather Solitons

Setting $H(y)=0$, $P(x,t)=\mathrm{e}^{-K^2t}\sin(Kx)$ and $Q(y)=N\sin(\ln(y^2))(1-\sin(\ln(y^2)))$ in Eqs. (7) reduces them to:

$$\begin{cases} u_2(x,y,t)=K\mathrm{e}^{-K^2t}\cos(Kx)[1+MN\sin(\ln(y^2))(1-\sin(\ln(y^2)))]/[C+\mathrm{e}^{-K^2t}\sin(Kx) \\ \quad +N\sin(\ln(y^2))(1-\sin(\ln(y^2)))+MN\mathrm{e}^{-K^2t}\sin(Kx)\sin(\ln(y^2))\cdot(1-\sin(\ln(y^2)))], \\ v_2(x,y,t)=\dfrac{2N\cos(\ln(y^2))(1-2\sin(\ln(y^2)))}{y}[1+M\mathrm{e}^{-K^2t}\sin(Kx)]/[C+\mathrm{e}^{-K^2t}\sin(Kx) \\ \quad +N\sin(\ln(y^2))(1-\sin(\ln(y^2)))+MN\mathrm{e}^{-K^2t}\sin(Kx)\sin(\ln(y^2))\cdot(1-\sin(\ln(y^2)))]. \end{cases} \tag{13}$$

Figure 2 shows a second coherent structure, which is symmetric about the plane y = 0 and periodic in the x-direction.



(a) 3-dimensional plot of $u_2(x, y, t)$ (b) Contour plot of $u_2(x, y, t)$

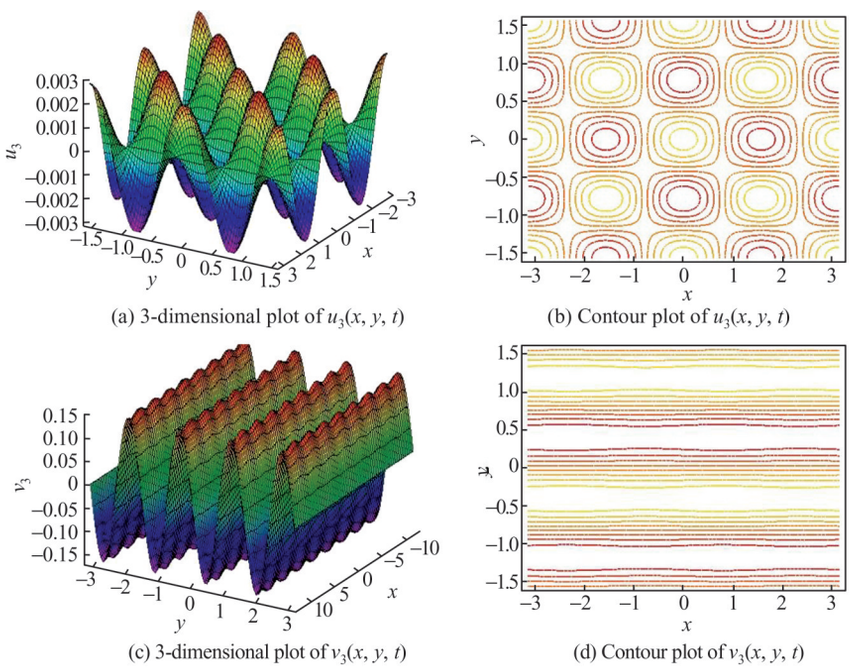
Fig. 2 Plots of $u_2(x,y,t)$ when $C=100$, $M=2$, $N=4$, $K=4$ and $t=1$ in Eqs. (13)

2.3 Double-Period Waves

Setting $P(x,t)=\mathrm{e}^{(-k_1^2t)}\sin(k_1x+x_0)$, $G(y)=\cos(k_2y+y_0)$ in Eqs. (10) gives:

$$\begin{cases} u_3(x,y,t)=\dfrac{C_0Mk_1\mathrm{e}^{(-k_1^2t)}\cos(k_1x+x_0)\cos(k_2y+y_0)}{K+C_0\cos(k_2y+y_0)+C_0M\mathrm{e}^{(-k_1^2t)}\cos(k_2y+y_0)\sin(k_1x+x_0)}, \\ v_3(x,y,t)=\dfrac{C_0k_2\sin(k_1x+x_0)[1+M\mathrm{e}^{(-k_1^2t)}\sin(k_1x+x_0)]}{K+C_0\cos(k_2y+y_0)+C_0M\mathrm{e}^{(-k_1^2t)}\cos(k_2y+y_0)\sin(k_1x+x_0)}. \end{cases} \tag{14}$$

The solutions are periodic in both x and y, with smallest positive periods $\dfrac{2\pi}{|k_1|}$ and $\dfrac{2\pi}{|k_2|}$, respectively. Figure 3 shows the resulting double-periodic wave structures.



(a) 3-dimensional plot of $u_3(x, y, t)$ (b) Contour plot of $u_3(x, y, t)$

(c) 3-dimensional plot of $v_3(x, y, t)$ (d) Contour plot of $v_3(x, y, t)$

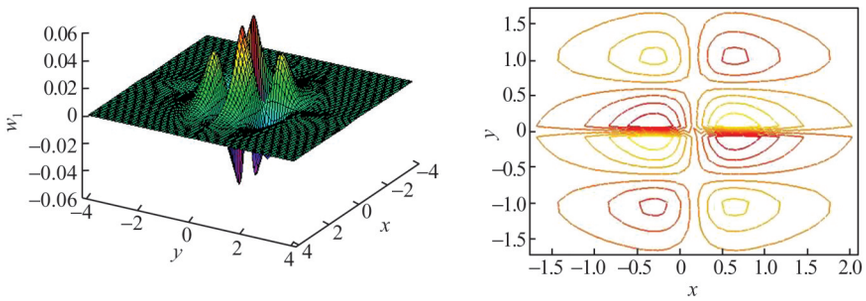
Fig. 3 Plots of $u_3(x,y,t)$ and $v_3(x,y,t)$ when $K=100$, $M=2$, $C_0=4$, $k_1=2$, $k_2=4$, $x_0=0$, $y_0=0$ and $t=1$ in Eqs. (14)

3 The Local Structure of $w(x, y, t)$ for Eqs. (1)

Since $w(x,y,t)=u_y=v_x$, this quantity reflects both the physical properties of the system and the corresponding changes in $u(x,y,t)$ and $v(x,y,t)$. Therefore, $w(x,y,t)$ can be used to simplify the problem and to construct new solutions[22]. With suitable choices of $P(x,t)$ and $Q(y)$ in Eq. (8), $w(x,y,t)$ acquires novel local structures, such as fractal structures and chaotic patterns[34].

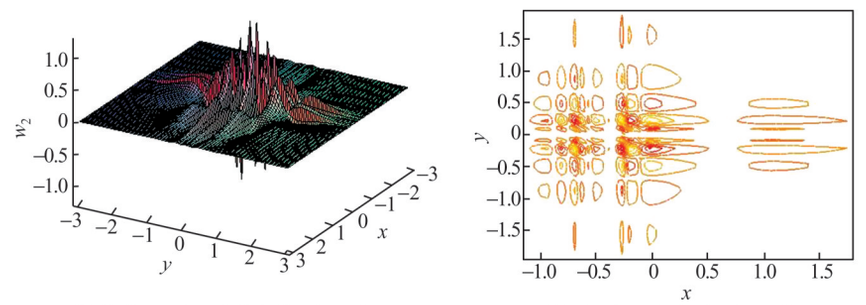
3.1 Fractal Rogue Waves

With $C=100$, $M=2$, $P(x,t)=2\mathrm{e}^{(4t+2x)}+4\mathrm{e}^{(4t-2x)}$ and $Q(y)=1+\dfrac{|y|\cos(\ln(1+y^2))^2}{1+y^4}$, Eq. (8) yields a fractal rogue wave $w_1(x,y,t)$, plotted in Fig. 4. Taking $P(x,t)=1+\dfrac{|2x+4t|\cos[\ln((2x+4t)^2)+\sin((2x+4t)^2)]}{1+x^4}$ and $Q(y)=1+\dfrac{|y|[\cos(\ln(1+y^2))+\sin(\ln(1+y^2))]^2}{1+y^4}$ instead yields a second fractal rogue wave $w_2(x,y,t)$, shown in Fig. 5. The two profiles differ in how the pattern is distributed. In Fig. 4(b), the closed contours form four groups placed symmetrically above and below $y = 0$ and are linked by a narrow ridge along $y = 0$. In Fig. 5(b), they spread over the whole window and become smaller and more closely spaced toward $x = 0$, with the same sequence of scales repeated on either side. This self-similarity comes from the factors $\cos[\ln(1 + y^2)]$ and $\cos[\ln((2x + 4t)^2)]$, which are periodic in the logarithm of their argument and therefore reproduce the same profile at geometrically spaced scales.



(a) 3-dimensional plot of $w_1(x, y, t)$ (b) Contour plot of $w_1(x, y, t)$

Fig. 4 Plots of $w_1(x, y, t)$ when $t = 1$

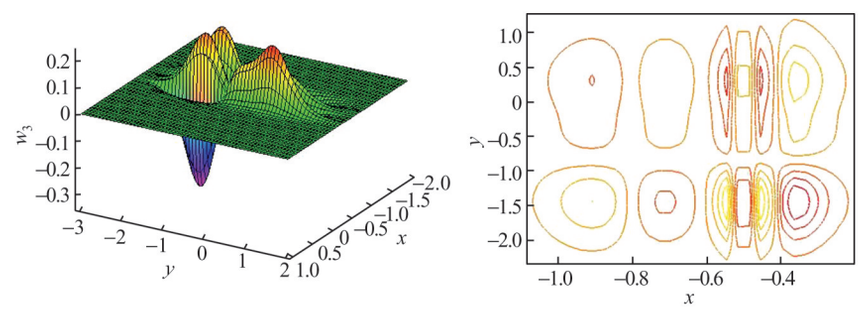


(a) 3-dimensional plot of $w_2(x, y, t)$ (b) Contour plot of $w_2(x, y, t)$

Fig. 5 Plots of $w_2(x, y, t)$ when $t = 1$

3.2 Fractal Dromion

In Eq. (8), setting $P(x,t)=1+e^{[-(2x+4t)(2x+4t+\sin(\ln((2x+4t)^2))+\cos(\ln((2x+4t)^2)))]}$, $C=100$, $M=2$ and $Q(y)=1+e^{[-y(y+\sin(\ln(1+y^2))+\cos(\ln(1+y^2)))]}$ yields a fractal dromion $w_3(x,y,t)$, plotted in Fig. 6. Unlike the profiles in Figs. 4 and 5, this one is localized in both x and y: the exponent in each factor is quadratic in its argument, so the profile decays away from the line $2x + 4t = 0$ and from $y = 0$. In Fig. 6(b), the closed contours form two columns of nested squares, and their linear size falls by a constant ratio at each level of nesting, with the same ratio recurring above and below $y = 0$.

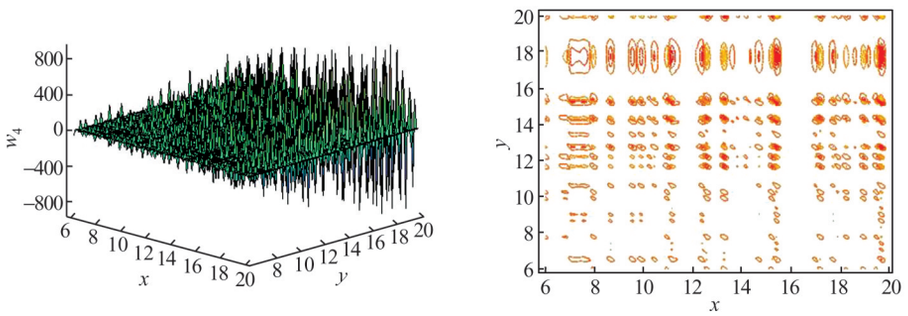


(a) 3-dimensional plot of $w_3(x, y, t)$ (b) Contour plot of $w_3(x, y, t)$

Fig. 6 Plots of $w_3(x, y, t)$ when $t = 1$

3.3 Chaotic Pattern

With $C=100$, $M=2$, $P(x,t)=[1-\frac{1}{\frac{3}{2}+\sin((2x+3t)^2)}]/[\frac{1}{\frac{3}{2}+\sin((2x+3t)^2)}]$ and $Q(y)=[1-\frac{1}{\frac{3}{2}+\sin(y^2)}]/[\frac{1}{\frac{3}{2}+\sin(y^2)}]$, Eq. (8) yields a chaotic pattern $w_4(x,y,t)$, plotted in Fig. 7. The profile has no period in x or y, and because its local wavenumber grows as $|x|$ increases, no two portions of the pattern repeat. The phases enter as $(2x + 3t)^2$ and y^2 rather than linearly, so the local wavenumber is $4(2x + 3t)$ with respect to x and $2y$ with respect to y; this is why the contours in Fig. 7(b) are sparse near $x = 6$ and crowded near $x = 20$.



(a) 3-dimensional plot of $w_4(x, y, t)$ (b) Contour plot of $w_4(x, y, t)$

Fig. 7 Plots of $w_4(x, y, t)$ when $t = 1$

4 Conclusion

In this study we combined the auxiliary equation mapping method with the homogeneous balance method and obtained variable separation solutions of the BLP equation. These solutions provide a basis for constructing new coherent structures and for analyzing the local structure of the associated physical quantities. The structures obtained here extend the known solution set of the BLP equation, and the fractal and chaotic cases show how varied its dynamics can be. Further work may consider more general combinations of the arbitrary functions in order to generate additional solutions. The present study is restricted to the existence and the structural features of exact solutions; their dynamical stability and physical applications remain open.

References

[1] Boiti M, Leon J J P, Pempinelli F. Integrable two-dimensional generalisation of the sine- and sinh-Gordon equations[J]. *Inverse Problems*, 1987, **3**(1): 37-49.

[2] Jiang Y, Tian B, Liu W J, *et al*. Solitons, Bäcklund transformation and Lax pair for the (2+1)-dimensional Boiti-Leon-Pempinelli equation for the water waves[J]. *Journal of Mathematical Physics*, 2010, **51**: 093519.

[3] Singh M. A revisit of symmetry analysis and group classifications of Boiti-Leon-Pempinelli system in (2+1) -dimensions[J]. *International Journal of Applied and Computational Mathematics*, 2022, **8**(2): 49.

[4] Ghazanfar S, Ahmed N, Iqbal M S, *et al*. Analysis of multi-wave solitary solutions of (2+1) -dimensional coupled system of Boiti-Leon-Pempinelli[J]. *Scientific Reports*, 2024, **14**: 20234.

[5] Sil S, Raja Sekhar T. Nonlocal conservation laws and dynamics of soliton solutions of (2+1)-dimensional Boiti-Leon-Pempinelli system[J]. *Physics of Fluids*, 2022, **34**(11): 117113.

[6] Radha R, Singh S, Kumar C S, *et al*. Elusive exotic structures and their collisional dynamics in (2+1) -dimensional Boiti-Leon-Pempinelli equation[J]. *Physica Scripta*, 2022, **97** (12): 125211.

[7] Seadawy A R, Ali A, Helal M A. Analytical wave solutions of the (2+1) -dimensional Boiti-Leon-Pempinelli and Boiti-Leon-Manna-Pempinelli equations by mathematical methods [J]. *Mathematical Methods in the Applied Sciences*, 2021, **44** (18): 14292-14315.

[8] Yang Z, Ma S H, Fang J P. Soliton excitations and chaotic patterns for the (2+1) -dimensional Boiti-Leon-Pempinelli system[J]. *Chinese Physics B*, 2011, **20**(6): 060506.

[9] Wu H Y, Jiang L H. Instruction on the construction of coherent structures based on variable separation solutions of (2+1) -dimensional nonlinear evolution equations in fluid mechanics[J]. *Nonlinear Dynamics*, 2019, **97**(1): 403-412.

[10] Zhao Z L, Han B. Lie symmetry analysis Bäcklund transformations and exact solutions of a (2+1) -dimensional Boiti-Leon-Pempinelli system[J]. *Journal of Mathematical Physics*, 2017, **58**(10): 101514.

[11] Radha R, Lakshmanan M. Exotic coherent structures in the (2+1) -dimensional long dispersive wave equation[J]. *Journal of Mathematical Physics*, 1997, **38**(1): 292-299.

[12] Wazwaz A M, Mehanna M S. A variety of exact travelling wave solutions for the (2+1) -dimensional Boiti-Leon-Pempinelli equation[J]. *Applied Mathematics and Computation*, 2010, **217**(4): 1484-1490.

[13] Huang D J, Zhang H Q. Exact travelling wave solutions for the Boiti-Leon-Pempinelli equation[J]. *Chaos Solitons & Fractals*, 2004, **22**(1): 243-247.

[14] Ren Y J, Liu S T, Zhang H Q. A new generalized algebra method and its application in the (2+1) dimensional Boiti-Leon-Pempinelli equation[J]. *Chaos Solitons & Fractals*,

2007, **32**(5): 1655-1665.

[15] El-Shiekh R M. Periodic and solitary wave solutions for a generalized variable-coefficient Boiti-Leon-Pempinlli system [J]. *Computers & Mathematics with Applications*, 2017, **73** (7): 1414-1420.

[16] Baskonus H M, Bulut H. Exponential prototype structures for (2+1) -dimensional Boiti-Leon-Pempinelli systems in mathematical physics[J]. *Waves in Random and Complex Media*, 2016, **26**(2): 189-196.

[17] Yu J Q, Liu X Q, Wang T T. Exact solutions and conservation laws of (2+1)-dimensional Boiti-Leon-Pempinelli equation[J]. *Applied Mathematics and Computation*, 2010, **216** (8): 2293-2300.

[18] Ma W X. Diversity of exact solutions to a restricted Boiti-Leon-Pempinelli dispersive long-wave system[J]. *Physics Letters A*, 2003, **319**(3): 325-333.

[19] Fei J X, Ma Z Y, Chen Y M. Symmetry reduction and explicit solutions of the (2+1) -dimensional Boiti-Leon-Pempinelli system[J]. *Applied Mathematics and Computation*, 2015, **268**: 432-438.

[20] Tang X Y, Lou S Y. Extended multilinear variable separation approach and multivalued localized excitations for some (2+1)-dimensional integrable systems[J]. *Journal of Mathematical Physics*, 2003, **44**(9): 4000-4025.

[21] Lu Z S, Zhang H Q. Soliton like and multi-soliton like solutions for the Boiti-Leon-Pempinelli equation[J]. *Chaos Solitons & Fractals*, 2004, **19**(3): 527-531.

[22] Mu G, Dai Z D, Zhao Z H. Localized structures for (2+1)-dimensional Boiti-Leon-Pempinelli equation[J]. *Pramana*, 2013, **81**(3): 367-376.

[23] Wang G W, Vega-Guzman J, Biswas A, *et al*. (2+1)-dimensional Boiti-Leon-Pempinelli equation—Domain walls, invariance properties and conservation laws[J]. *Physics Letters A*, 2020, **384**(10): 126255.

[24] Weiss J. Factorization of the (2+1)-dimensional BLP integrable system by the periodic fixed points of its Bäcklund transformations[J]. *Physics Letters A*, 1991, **160**(2): 161-165.

[25] Kumar M, Kumar R. On new similarity solutions of the Boiti-Leon-Pempinelli system[J]. *Communications in Theoretical Physics*, 2014, **61**(1): 121-126.

[26] Kumar M, Kumar R, Kumar A. Some more similarity solutions of the (2+1)-dimensional BLP system[J]. *Computers and Mathematics with Applications*, 2015, **70**(3): 212-221.

[27] Dai C Q, Wang Y Y. Periodic structures based on variable separation solution of the (2+1) -dimensional Boiti-Leon-Pempinelli equation[J]. *Chaos Solitons & Fractals*, 2009, **39** (1): 350-355.

[28] Aslan I. Application of the Exp-function method to the (2+1)-dimensional Boiti-Leon-Pempinelli equation using symbolic computation[J]. *International Journal of Computer Mathematics*, 2011, **88**(4): 747-761.

[29] Ni W G, Dai C Q. Note on same result of different ansatz based on extended tanh-function method for nonlinear models[J]. *Applied Mathematics and Computation*, 2015, **270**: 434-440.

[30] Feng W G, Li K M, Li Y Z, *et al*. Explicit exact solutions for (2+1)-dimensional Boiti-Leon-Pempinelli equation[J]. *Communications in Nonlinear Science and Numerical Simulation*, 2009, **14**(5): 2013-2017.

[31] Fang J P, Zheng C L, Zhu J M. New variable separation excitations, rectangle-like solitons and fractal solitons in the Boiti-Leon-Pempinelli system[J]. *Acta Physica Sinica*, 2005, **54**(7): 2990-2995.

[32] Ma S H, Xu G H, Zhu H P. Complex solutions and novel complex wave localized excitations for the (2+1) -dimensional Boiti-Leon-Pempinelli system[J]. *Chinese Physics B*, 2014, **23**(5): 050511.

[33] Li Z T. New coherent structures and interaction behavior for the new (2+1)-dimensional Korteweg de Vries equation[J]. *Chaos Solitons & Fractals*, 2024, **184**: 115007.

[34] Ma S H, Fang J P, Zheng C L. Complex wave excitations and chaotic patterns for a general (2+1) -dimensional Korteweg-de Vries system[J]. *Chinese Physics B*, 2008, **17** (8): 2767-2773.

（2+1）维Boiti-Leon-Pempinelli方程的新相干结构与混沌斑图

刘常福

文山学院 人工智能学院，云南 文山 663099

摘要：（2+1）维Boiti-Leon-Pempinelli（BLP）方程具有可积性，且存在大量超越经典孤子的相干结构，但这类结构难以通过系统性方法推导得到。本文将辅助方程映射法与齐次平衡法相结合，得到了含两个任意函数的可分离变量解。借助这两个任意函数，本文在同一框架内构造了呼吸双孤子、对称呼吸孤子与双周期波。对相应势场的分析进一步表明，由奇异流形可诱导出分形怪波、分形dromion与混沌斑图。可见，任意函数的选取直接决定所得的动力学行为，这有助于阐明BLP方程的相干机制。

关键词：（2+1）维Boiti-Leon-Pempinelli方程；辅助方程映射法；可分离变量解；相干结构；混沌斑图

□